

## Finite-Element Solution of Navier-Stokes Equations for Transient Two-Dimensional Incompressible Flow

S. L. SMITH\* AND C. A. BREBBIA†

*Department of Civil Engineering, University of Southampton, England*

Received January 22, 1974; revised July 17, 1974

A method is described for the solution of transient, incompressible viscous flow in two dimensions. The dependent variables, stream function and vorticity, were approximated over each triangular element using linear interpolation functions. This approximation reduces the problem to a set of matrix equations whose term involving derivatives of time is the mass matrix. The lumping of this matrix together with the application of Euler integration scheme produces an efficient method of solution. Once the nodal values of the stream function are known the velocities and pressure can be computed.

As an application a study of the vortex street development behind a rectangular obstruction is described. The flow has been impulsively accelerated to a constant speed in a channel of finite width. The Reynolds number range investigated is between 20 and 100.

### INTRODUCTION

Many efforts have been made to integrate the nonlinear partial differential equations known as the Navier-Stokes equations. In the last 10 years, however, applications of finite-difference and finite-element approximations, together with high-speed digital computers have proved successful in solving these equations for special cases of geometry and flow.

A finite-difference scheme presented by Fromm and Harlow in [1] has had considerable success in solving problems for which flow is unstable, but in addition to having a regular mesh it seems to require large amounts of computer time. The need for a more versatile method has led several investigators to the application of the finite-element method to Navier-Stokes equations.

Tong [2] in 1971 presented results for steady flow using finite elements with pressure and velocities as dependent variables. Steady flow problems were also solved by Olson [3] who used stream function as the unknown, and high order elements.

Lieber *et al.* [4] have more recently presented results for steady flow using an

\* Research Assistant at Southampton University.

† Lecturer at Southampton University.

efficient stream function only with a finite-element formulation. They employ a nonfully compatible interpolation function which has been successfully used for plate bending. Oden [5, 6] developed a finite-element pressure-velocities formulation for both transient and steady nonuniform flow problems. A similar formulation has been presented by Lee [7] but in cylindrical coordinates.

Hood and Taylor [8] have also used the pressure-velocities formulation to study various steady flow problems at Re number up to 100. They have recently presented a formulation using higher order interpolation functions for velocities than pressure, which they claim to give more accurate pressure fields [9].

A solution based on stream and vorticity functions was carried out by Cheng [10] for the case of a constricted channel using a Eulerian-Lagrangian scheme which enables an implicit time integration scheme. Computations were only carried out to Reynolds number when separation was established. Baker [11] also solved the Navier-Stokes equations expressed in terms of vorticity and stream functions but referred to a Eulerian system of coordinates using an explicit predictor-corrector time integration scheme for steady flow configurations. In a recent paper [12] he presented results for transient flow ( $Re = 200$ ) up to a steady state solution.

For practical two-dimensional applications it is necessary to have a method which is as general as possible and also economic. In this paper this has been attempted using a vorticity and stream function formulation, which conserves mass identically, eliminates one degree of freedom when compared against the pressure-velocities approach and has no cross linking in time between the unknowns, due to a time delay approximation.

The solution strategy is similar to Baker's [11] but for the problem of vortex street development modifications were necessary to bring computer time and storage to an acceptable level. Hence the solution presented differs in the following ways.

- (a) Quadratic interpolation functions were replaced by linear ones.
- (b) A lumped mass system was used.
- (c) A simple Euler time integration scheme was used.

The solution was applied to the problem of vortex street development behind a rectangular obstruction in a channel of finite width. Results were compared against those presented in [1].

#### GOVERNING EQUATIONS

The governing equations for two-dimensional transient incompressible viscous flow can be written in terms of  $\psi$  stream function and  $\omega$  vorticity as

$$(\partial\omega/\partial t) + (\partial\psi/\partial y)(\partial\omega/\partial x) - (\partial\psi/\partial x)(\partial\omega/\partial y) = \nu\nabla^2\omega. \quad (1)$$

The relationship between  $\omega$  and  $\psi$  is given by

$$\omega = -\nabla^2\psi. \quad (2)$$

We will now propose to solve Eqs. (1) and (2) plus the corresponding boundary conditions. The natural boundary conditions for (1) and (2) are

$$\partial\omega/\partial n = g_\omega \text{ on } S_\omega \quad \text{and} \quad \partial\psi/\partial n = g_\psi \text{ on } S_\psi. \quad (3)$$

We can now write Eqs. (1)–(3) in a variational (Galerkin-type) statement [4] valid at any time  $t$ :

$$\begin{aligned} \iint \left( \frac{\partial\omega}{\partial t} + \frac{\partial\psi}{\partial y} \frac{\partial\omega}{\partial x} - \frac{\partial\psi}{\partial x} \frac{\partial\omega}{\partial y} - \nu\nabla^2\omega \right) \delta\psi \, dx \, dy &= \int_{S_\omega} \left( g_\omega - \frac{\partial\omega}{\partial n} \right) \delta\psi \, dS, \\ \iint (\nabla^2\psi + \omega) \delta\omega \, dx \, dy &= \int_{S_\psi} \left( \frac{\partial\psi}{\partial n} - g_\psi \right) \delta\omega \, dS. \end{aligned} \quad (4)$$

Integrating the  $\nabla^2$  terms by parts gives

$$\begin{aligned} \iint \left\{ \left( \frac{\partial\omega}{\partial t} + \frac{\partial\psi}{\partial y} \frac{\partial\omega}{\partial x} - \frac{\partial\psi}{\partial x} \frac{\partial\omega}{\partial y} \right) \delta\psi \right. \\ \left. + \nu \left( \frac{\partial\delta\psi}{\partial x} \frac{\partial\omega}{\partial x} + \frac{\partial\delta\psi}{\partial y} \frac{\partial\omega}{\partial y} \right) \right\} dx \, dy &= \int_{S_\omega} g_\omega \delta\psi \, dS, \\ \iint \left\{ -\frac{\partial\delta\omega}{\partial x} \frac{\partial\psi}{\partial x} - \frac{\partial\delta\omega}{\partial y} \frac{\partial\psi}{\partial y} + \omega \delta\omega \right\} &= - \int_{S_\psi} g_\psi \delta\omega \, dS. \end{aligned} \quad (5)$$

#### FINITE-ELEMENT SOLUTION

We will divide the continuum into a number of three nodes triangular elements [15] and assume on each of them that the  $\omega$  and  $\psi$  functions can be approximated by

$$\omega = \boldsymbol{\varphi}^T \boldsymbol{\omega}^n, \quad \psi = \boldsymbol{\varphi}^T \boldsymbol{\psi}^n. \quad (6)$$

$\boldsymbol{\varphi}$  is the interpolation function (the same for  $\omega$  and  $\psi$  in this case) and  $\boldsymbol{\omega}^n$ ,  $\boldsymbol{\psi}^n$  are the nodal values of vorticity and stream functions.

Substitution of (6) into (5) gives,

$$\begin{aligned} \delta\boldsymbol{\psi}^{n,T} \{ \mathbf{M}\dot{\boldsymbol{\omega}}^n + \mathbf{A}\boldsymbol{\omega}^n + \nu\mathbf{K}\boldsymbol{\omega}^n - \mathbf{B}_\omega \} &= 0, \\ \delta\boldsymbol{\omega}^{n,T} \{ \mathbf{K}\boldsymbol{\psi}^n - \mathbf{B}_\psi + \mathbf{M}\boldsymbol{\omega}^n \} &= 0, \end{aligned} \quad (7)$$

where

$$\begin{aligned} \mathbf{M} &= \iint \boldsymbol{\varphi} \boldsymbol{\varphi}^T dx dy, \\ \mathbf{A} &= \iint \boldsymbol{\varphi} \left\{ \left( \frac{\partial \boldsymbol{\varphi}}{\partial y} \right)^T \boldsymbol{\psi}^n \left( \frac{\partial \boldsymbol{\varphi}}{\partial x} \right)^T - \left( \frac{\partial \boldsymbol{\varphi}}{\partial x} \right)^T \boldsymbol{\psi}^n \left( \frac{\partial \boldsymbol{\varphi}}{\partial y} \right)^T \right\} dx dy, \\ \mathbf{K} &= \iint \left\{ \frac{\partial \boldsymbol{\varphi}}{\partial x} \left( \frac{\partial \boldsymbol{\varphi}}{\partial x} \right)^T + \frac{\partial \boldsymbol{\varphi}}{\partial y} \left( \frac{\partial \boldsymbol{\varphi}}{\partial y} \right)^T \right\} dx dy, \\ \mathbf{B}_\omega &= \int_{S_\omega} \boldsymbol{\varphi} g_\omega dS, \\ \mathbf{B}_\psi &= \int_{S_\psi} \boldsymbol{\varphi} g_\psi dS. \end{aligned} \quad (8)$$

Equations (7) hold for any arbitrary variation  $\delta\omega$  or  $\delta\psi$ . Hence we have, for one element,

$$\begin{aligned} \mathbf{M}\dot{\boldsymbol{\omega}}^n + \mathbf{A}\boldsymbol{\omega}^n + \nu\mathbf{K}\boldsymbol{\omega}^n &= \mathbf{B}_\omega, \\ \mathbf{K}\boldsymbol{\psi}^n &= \mathbf{B}_\psi - \mathbf{M}\boldsymbol{\omega}^n. \end{aligned} \quad (9)$$

Before assembling the elements we will "lump" the mass matrix in order to diagonalize them. This is done because it enables considerable savings in computer time and it has been proved very successful in other dynamic problems. The lumping consists in distributing the mass of the elements equally at the three corner nodes. Thus (9) becomes

$$\begin{aligned} \mathbf{M}^*\dot{\boldsymbol{\omega}}^n + \mathbf{A}\boldsymbol{\omega}^n + \nu\mathbf{K}\boldsymbol{\omega}^n &= \mathbf{B}_\omega, \\ \mathbf{K}\boldsymbol{\psi}^n &= \mathbf{B}_\psi - \mathbf{M}^*\boldsymbol{\omega}^n, \end{aligned} \quad (10)$$

where  $\mathbf{M}^*$  are the diagonalized mass matrices.

We can now assemble all the elements together and obtain, for the whole continuum,

$$\mathbf{M}\dot{\boldsymbol{\Omega}} + \mathbf{A}\boldsymbol{\Omega} + \nu\mathbf{K}\boldsymbol{\Omega} = \mathbf{B}_\omega, \quad (11)$$

$$\mathbf{K}\boldsymbol{\Phi} = \mathbf{B}_\psi - \mathbf{M}\boldsymbol{\Omega}. \quad (12)$$

We will also assume that the essential boundary conditions have been applied in Eq. (11) and integrate them in time. For this integration the simple Euler scheme was used which gives a recurrence relationship of the following type for Eq. (11).

$$\boldsymbol{\Omega}_{t+\Delta t} = \boldsymbol{\Omega}_t + \Delta t \mathbf{M}^{-1} \{ -\mathbf{A}\boldsymbol{\Omega} - \nu\mathbf{K}\boldsymbol{\Omega} + \mathbf{B}_\omega \}. \quad (13)$$

$\Delta t$ : time increment.

The term  $\mathbf{A}$  which is function of  $\Phi$  can be found by solving Eq. (12) with the  $\Omega$  values at time  $t$ , i.e.,

$$\Phi = \mathbf{K}^{-1}(\mathbf{B}_\psi - \mathbf{M}\Omega_t). \quad (14)$$

The vorticity along a no-slip boundary may be evaluated as follows. For elements situated on the no-slip boundaries the stream function is constant along the wall. Hence Eq. (2) may be integrated some distance normal to the wall (note that it becomes an ordinary differential equation). Using the three node element (linear variation) the integral may be evaluated directly giving

$$\Omega_{\text{wall}} = -[(3(\Phi - \Phi_{\text{wall}})/l^2) + (\Omega/2)] \quad (15)$$

$l$ : distance normal to the wall.

Thus we can evaluate the vorticity at the wall in terms of the wall stream function and an interior value of both stream function ( $\Phi$ ) and vorticity ( $\Omega$ ), located at the distance  $l$  normal to the wall.

The method of solution consists of the following steps.

- (a) Evaluation of stream functions at  $t + \Delta t$  using Eq. (14): The values of vorticities except on the nonslip boundaries being those from the previous time step " $t$ " or in particular the initial conditions. On the nonslip boundaries the wall vorticities are from the  $t - \Delta t$  cycle or an initial estimate.
- (b) Equation (15) is used to correct the wall vorticity values.
- (c) The stream function values are substituted in Eq. (13) to find the vorticities at  $t + \Delta t$ .

The above procedure has to be repeated for as many  $\Delta t$  as required. Each step implies a new evaluation of Eq. (13) which shows the convenience of employing a lumped mass system, for which  $\mathbf{M}$  is a diagonal matrix and its inverse is immediate.

#### APPLICATIONS

The above formulation has been applied to study flow in a channel of finite width a rectangular obstruction. The channel is 4.5 m long and 1 m width. The obstruction was situated 1.05 m from the channel entrance and was 0.4 m long by 0.166 m (Fig. 1). The initial viscosity was taken as 0.01666 m<sup>2</sup>/sec.

The fluid was instantaneously accelerated by applying a uniform velocity of 2.0 m/sec upstream of the channel. As an approximation, the vorticity initially was taken as zero everywhere in the interior of the domain. For uniform flow at

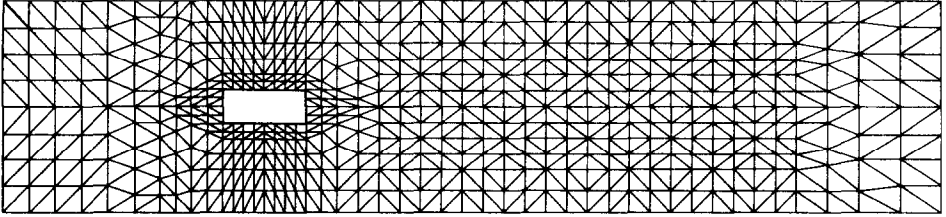


FIG. 1. Finite-element mesh.

the channel entrance the vorticity is zero and the stream function is a linear function of the  $y$  coordinate. The normal derivatives of the vorticity and stream function are both zero at the exit enforcing parallel flow. The values of the stream function along the upper and lower wall and along the boundary of the obstruction are constant and equal to 2.0, 0.0, and 1.0  $m^2/sec$ , respectively (see Fig. 2).

Figure 3 shows the streamlines and vorticities in the region to the obstruction at a time  $t = 2.85$  sec. This was the time required to reach the “statistically steady

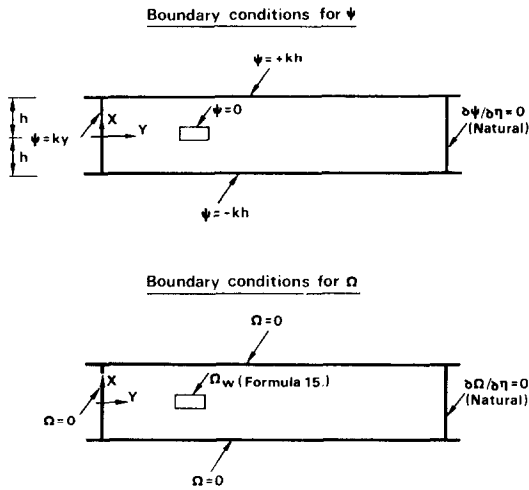


FIG. 2. Boundary conditions.

state” as defined by Baker [11], i.e., when the largest value of  $\partial\omega/\partial t$  at any node decreases to 0.04. The Reynolds number for this example taken with respect to the width of the obstruction was equal to 20 and the initial vorticity distributed equal to zero. At  $t = 2.85$  sec the viscosity was instantaneously decreased by 60% giving a Reynolds number of 50. The time step was reduced in an inversely proportional ratio to the Reynolds number. Figure 4 shows the stream function and

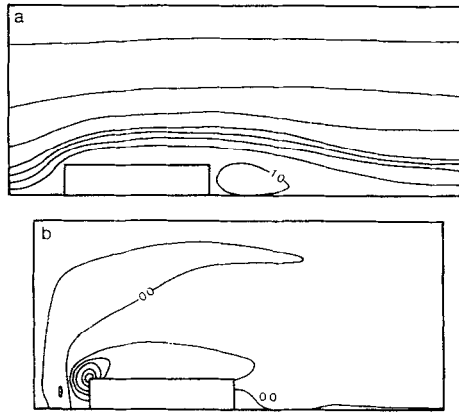


FIG. 3. (a) Streamlines for  $Re = 20$ ; (b) Vorticity functions for  $Re = 20$ ;

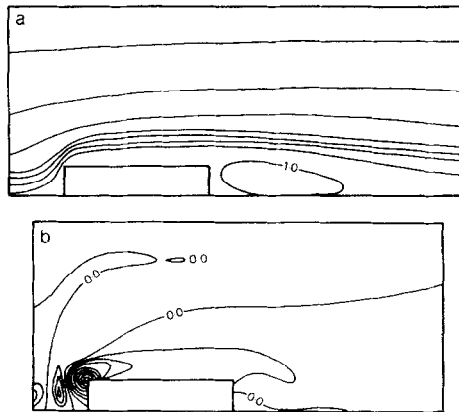


FIG. 4. (a) Streamlines for  $Re = 50$ ; (b) Vorticity functions for  $Re = 50$ .

vorticity at the time  $t = 11.5$  sec when the statistically steady state has been reached. At this time the viscosity was again reduced by a further 50% within 0.33 sec. Figure 5 shows the streamlines and vorticity at  $t = 17.5$  sec. At this stage the value of  $\partial\omega/\partial t$  showed no sign of decreasing to the value of 0.04. The time step for this case was also found by reducing the original time step in an inversely proportional ratio to the  $Re$  number. This criterion was found to produce an overreduction for large  $Re$  numbers.

Instabilities, inherent in numerical solution of the momentum equations at this Reynolds number and propagated by computer round-off error, eventually

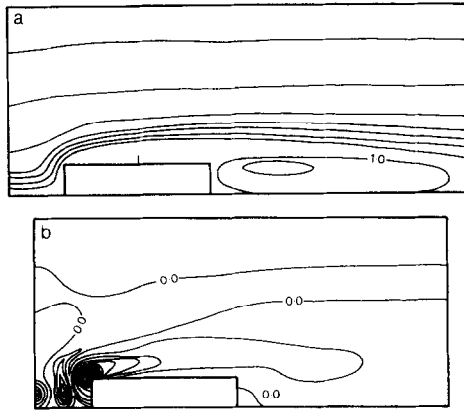


FIG. 5. (a) Streamlines for  $Re = 100$ ; (b) Vorticity functions for  $Re = 100$ .

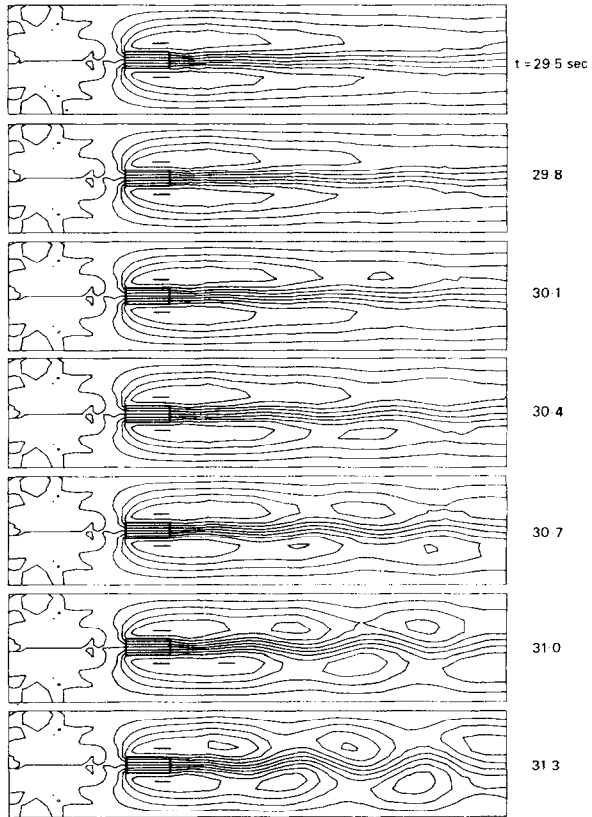


FIG. 6. Vortex street development for  $Re = 100$  (Stationary streamlines). Lumped mass case.



increased until vortex shedding occurred. Figure 6 (from  $t = 29.5$  to  $31.3$  sec) shows this phenomenon, each frame being  $0.3$  sec apart. In order to show the vortex more clearly the free-flow streamline values were subtracted from the computed streamline values. The vortices are rather weak, which may be due to the long nature of the obstruction and the coarseness of the mesh. Because of the obstruction length very low values of velocities and vorticity were recorded at the downstream corners. The lumping of the mass together with the coarseness of the mesh produces an artificial damping effect destroying the angular momentum of the fluid. Nevertheless, the *STROUHAL* number (defined as the shedding frequency multiplied by the width of the obstruction divided by the free stream velocity) calculated from these results is approximately  $S = 0.12$ , which agrees favorably with that obtained by Fromm and Harlow [1],  $S = 0.119$  for the same Reynolds number 100.

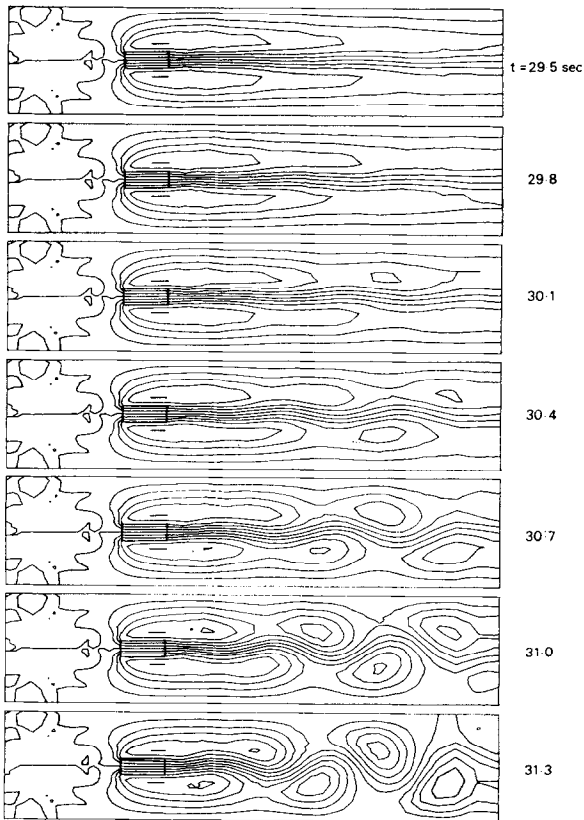


FIG. 7. Vortex street development for  $Re = 100$  (Stationary streamlines). Consistent mass case.

The ratio of vortex speed to wall speed (0.79 for a  $Re = 100$ ) was also found to be the same as the ratio reported in [1].

In order to find out the difference in results produced by the lumping of the masses, the same example was run without lumping the masses (i.e., consistent mass case). The results for  $Re = 100$  are shown in Fig. 7. Comparison with the previous results (Fig. 6) shows that although the lumping of the masses introduces a certain amount of damping, it does not change the overall flow configuration, i.e., the STROUHAL number and ratio of vortex speed to wall speed remains constant. Numerical tests indicate that this damping effect tends to diminish as  $t$  approaches infinity. The computer time ratio for the results shown in Figs. 6 and 7 is approximately 6 to 10.

Due to the inherent instability of the explicit time integration method, the time step used was very small. For  $Re = 20, 50,$  and  $100$ , the step was  $t = 0.01, 0.005,$  and  $0.0025$  sec, respectively. These are intermediate Reynolds numbers and neither the viscosity nor the velocity will govern the problem. For reference purposes we can summarize the parameters in Table I.

TABLE I<sup>a</sup>

	Reynolds number		
	20 ( $\Delta t = 0.01$ sec)	50 ( $\Delta t = 0.005$ sec)	100 ( $\Delta t = 0.0025$ sec)
$\nu\Delta t/(\Delta x)^2$	0.0666	0.0132	0.0033
$v\Delta t/\Delta x$	0.40	0.20	0.10
Steady state	Reached	Reached	Not reached

<sup>a</sup>  $\Delta x$  (minimum value) is 0.05 m;  $v = 2$  m/sec.

The computer CPU time per cycle was approximately 0.75 sec on an ICL 1906A machine and the storage required was 50K words (two words were required to store a floating point number).

## CONCLUSIONS

A method for solving the transient, incompressible, viscous and two-dimensional Navier–Stokes equations using finite elements has been applied to the problem of vortex street development behind a rectangular obstruction. The results are sufficiently accurate to describe the overall flow configuration for Reynolds numbers up to 100.

The simple Euler integration scheme was found to be sufficiently accurate for this particular problem. For instance after the initial 200 time integration steps the difference between Euler and second-order Runge-Kutta was found to be in the order of 0.1% at any node.

The lumped mass simplification, although given an artificial damping to the system, has proved to be highly economic in computer time.

#### REFERENCES

1. J. E. FROMM AND F. HARLOW, *Phys. Fluids* **6** (1963), 975-982.
2. P. TONG, The finite-element method for fluid flow, in "Recent Advances in Matrix Methods of Structural Analysis and Design" (R. Gallagher *et al.*, Eds.), University of Alabama Press, 1971, pp. 787-808.
3. M. D. OLSON, Formulation of a variational principle: Finite-element method for viscous flows, in "Variational Methods in Engineering" (C. A. Brebbia and H. Tottenham, Eds.), Vol. I, Southampton University Press, 1973.
4. P. LIEBER, K. S. WEN, AND A. V. ATTIA, Finite-element methods as an aspect of the principle of maximum Uniformity, in "Proc. Int. Symposium on Finite-Element Methods in Flow Problems," held at Swansea, January 1974.
5. J. T. ODEN, *J. Eng. Mech. Div. Am. Soc. Civil Eng.* **96** (1970), 529-534.
6. J. T. ODEN AND I. CARTER-WELLFORD, *AIAA J.* (1972), 1590-1599.
7. C. H. LEE, Finite-element method for transient linear viscous flow problems, in "Numerical Methods in Fluid Dynamics," (C. Brebbia and J. J. Connor, Eds.), Pentech Press, London, 1974, pp. 140-152.
8. P. HOOD AND C. TAYLOR, Navier-Stokes equations using mixed interpolation, in "Proc. Int. Symposium on Finite-Element Methods in Flow Problems," held at Swansea, January 1974.
9. C. TAYLOR AND P. HOOD, A numerical solution of the Navier-Stokes equations using the finite-element method, in "Computers and Fluids Journal," Vol. 1, 1973, pp. 73-100.
10. R. T. CHENG, *Phys. Fluids* **15** (1972), 2098-2105.
11. A. J. BAKER, *Internat. J. Numer. Methods Engrg* **6** (1973), 89-101.
12. A. J. BAKER, A highly-stable explicit integration technique for computational continuum mechanics, in "Numerical Methods in Fluid Dynamics" (C. Brebbia and J. J. Connor, Eds.), Pentech Press, London, 1974, pp. 99-120.
13. P. TONG, On the solution of the Navier-Stokes equations in two-dimensional and axial symmetric problems, in "Proc. Int. Symposium on Finite-Element Methods in Flow Problems," held at Swansea, January 1974.
14. B. A. FINLAYSON, "The Method of Weighted Residuals and Variational Principles," Academic Press, New York, 1972.
15. C. A. BREBBIA AND J. J. CONNOR, "Fundamentals of Finite-Element Techniques for Structural Engineers," Butterworths, London, 1973.